
ABSTRACT

Rimming steel consists of Carbon approximately 0.08-0.09% and Manganese 0.40-0.50%. This grade contains high oxygen (ppm) level in the bath around 1000-1200 and 225-275 in ladle after tapping. Rimming grade steel is casted only through ingot teeming route. Rim thickness and Rimming duration are the main physical quality parameters of a rimming steel ingot.

Of all the parameters, the casting temperature of steel plays a very important role in determining the quality of rimming steel. Superheat is the temperature by which the ladle temperature exceeds the liquidus temperature of steel. The magnitude of superheat affects the rate of solidification of steel in mould, as a result of which, the rimming intensity gets affected, which in turn, affects the rim thickness. Therefore, the study of superheat-rimming intensity correlation is important in controlling the quality of rimming steel.

KEY WORDS: Rimming steel, Super heat, Rimming intensity, Rim thickness

INTRODUCTION

Based on the level of deoxidation, steels can be classified as killed, semi-killed and rimming steel. Killed steels are characterized by the highest level of deoxidation, maximum carbon content, negligible evolution of CO gas during solidification, free from blowholes and the formation of cavity on the top of the ingot after solidification, which culminates into yield loss.

Semi – killed are adequately deoxidized steels which are commonly used as structural steels. During solidification carbon monoxide gas is evolved which generates blowhole and porosity distributed throughout the ingot. These porosities compensate for the pipe defect which is found in killed steels. The porosities vanish during rolling. Hence, yield of semi – killed steels is close to 90 % which is more than that for killed ones ⁽¹⁾.

On the contrary, rimming steels are the least deoxidized steels and the carbon content in such steels is minimum. During solidification huge amount of gas is evolved which prevents the formation of primary pipe ⁽²⁾. But such vigorous evolution of gas gives rise to blowholes. Rimming steel gathers popularity due to a purely ferrite rim which

is formed at the periphery of the ingot and its quality determines the quality of rimming steel. Rimming steels are used for welding electrodes and buss-bars .

The structure of solidified ingots of three kinds of steel is as shown in Fig.1 ⁽³⁾

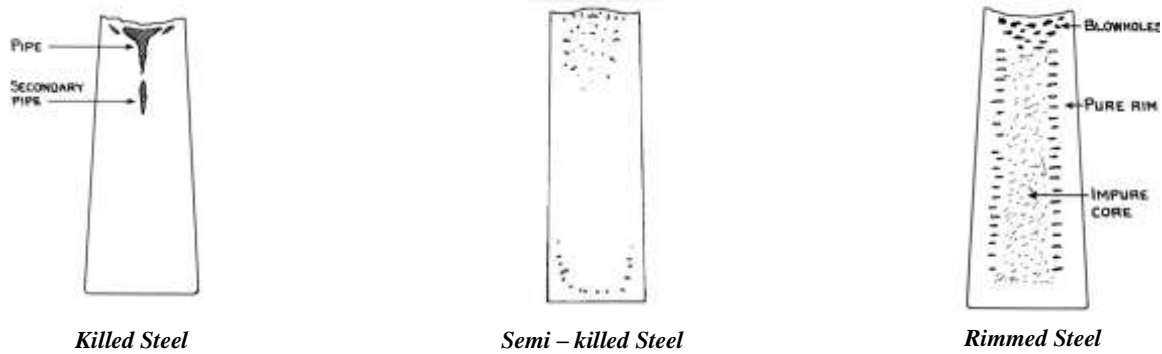


Fig.1 Structure of solidified ingots of steel

The most striking feature that makes rimming steels so popular is the presence of a skin on the ingot, whose thickness is known as “rim thickness” (Fig.2).

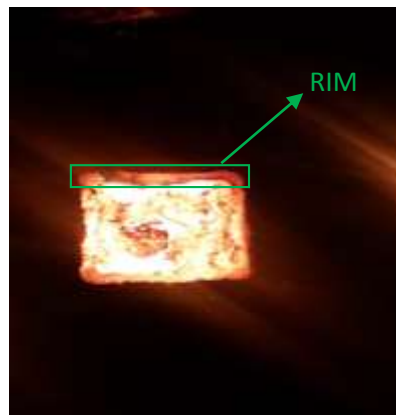


Fig. 2 Top view of a rimming steel ingot

Rim thickness is the distance from the periphery of the ingot till where the microstructure is purely ferrite (Fig. 3a). The microstructure of a rim comprises of ferrite. The carbon content in ferrite is ultra-low which imparts it ductility. On moving radially inwards towards the center of the ingot, the amount of ferrite decreases gradually and it is replaced by pearlite which has lamellar microstructure (Fig.3b). Another important property of the rim is its excellent conductivity of electricity due to its pure ferritic composition.

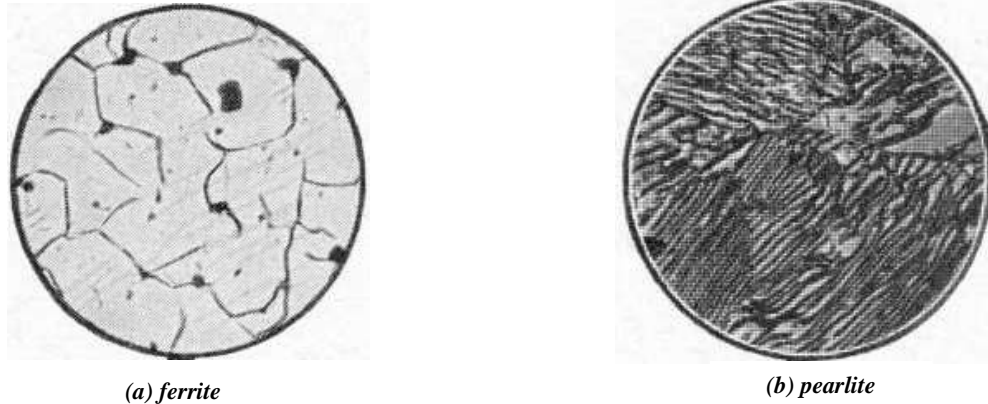


Fig. 3 Microstructure of different phases of steel

Studies have shown that among various parameters viz. Chemical composition (mainly C and Mn), oxygen content of steel, ladle temperature etc, the ladle temperature has a profound effect on the rimming action in mould ⁽⁴⁾. By controlling superheat, rim thickness can be regulated. The magnitude of superheat affects the rate of the solidification of steel in mould, as a result of which, the rimming intensity gets affected which in turn affects the rim thickness ⁽⁴⁾. Therefore, an attempt has been made to study the effect of ladle temperature on the rim thickness.

FACTORS AFFECTING RIM THICKNESS

Some of the important factors that affect rim thickness are Carbon, Oxygen, Manganese contents in steel, (C X O) of steel in ladle and ladle temperature ⁽⁴⁾. The ladle carbon content should not exceed 0.1 %, otherwise it would result into scarcity of oxygen, hence, poor rimming action ⁽⁴⁾. Adequate oxygen level for the ladle carbon content between 0.04 – 0.075 is between 250 – 300 ppm ⁽⁴⁾. Relation between C and O₂ content is expressed by the formula shown below ⁽²⁾

$$C \times O = 0.0025 - 0.0035 \quad (\text{steel}) \quad \text{Eq. (1)}$$

$$O = 0.015 + \frac{0.00175}{C} \quad (\text{mould}) \quad \text{Eq. (2)}$$

However, the availability of oxygen also depends on the manganese content, since, manganese acts as a deoxidizer. Therefore, an increase in the manganese content lowers the oxygen level resulting into poor rimming action. In case of teeming speed, low teeming speed enhances the soundness of rim because CO gas gets ample time to evolve. But, low teeming rate hampers productivity and also the temperature loss from steel in ladle. Therefore, teeming rate has to be optimum.

FACTORS AFFECTING THE LADLE TEMPERATURE

Tapping temperature of rimming steel is maintained around 1645°C⁽⁵⁾. However, due to ladle additions and due to the loss of heat through refractory, atmosphere and the time taken by the ladle to move from tapping side of the furnace to teeming bay, temperature drop takes place and the ladle temperature just before teeming comes down to somewhere between 1570 - 1595°C.

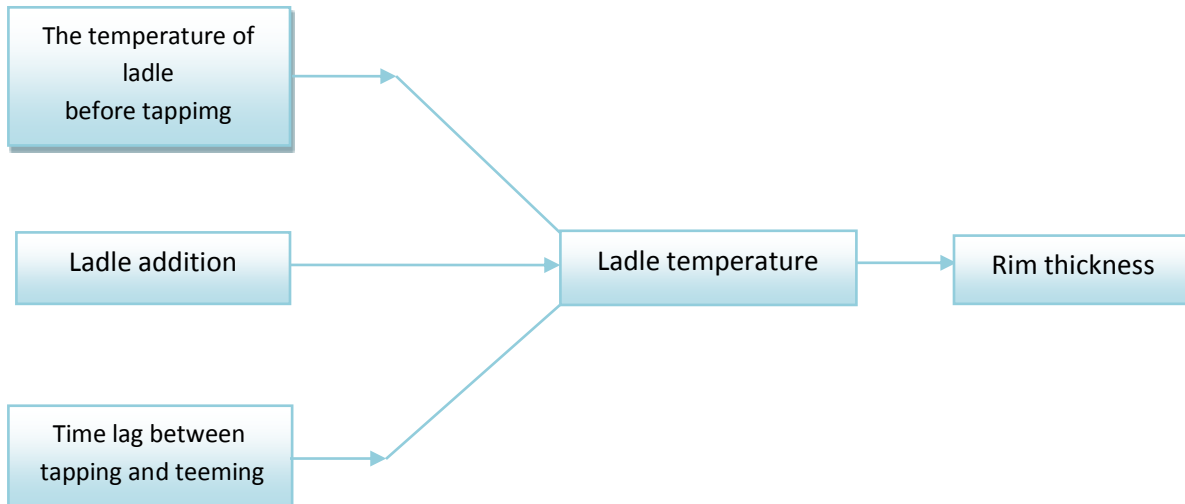


Fig.4 Factors leading to Ladle temperature and Rim thickness

EFFECT OF LADLE TEMPERATURE ON RIM THICKNESS

The ladle temperature effects rim thickness by affecting the rate of solidification and the ladle oxygen content⁽⁶⁾.

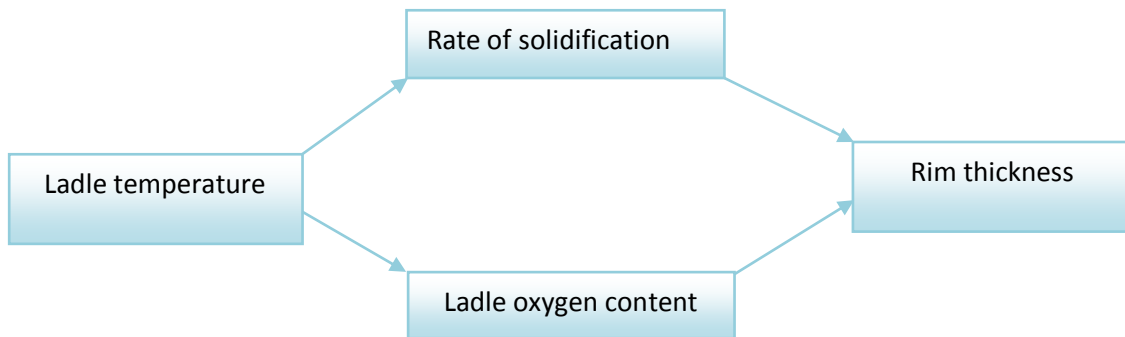


Fig.5 Effects of Ladle temperature leading to Rim thickness

The rate of solidification of steel in a mould depends, to a very large extent, on the ladle temperature. In order to achieve an optimum rate of solidification, the ladle temperature has to be taken care. Low rate of solidification leads to poor rimming action which is deleterious for the soundness of rim.

Heat transfer through the mould wall is expressed as below ⁽⁷⁾

$$\rho c \frac{\partial T}{\partial t} = \frac{\partial}{\partial x} \left(\lambda \frac{\partial T}{\partial x} \right) + \frac{\partial}{\partial y} \left(\lambda \frac{\partial T}{\partial y} \right) + \frac{\partial}{\partial z} \left(\lambda \frac{\partial T}{\partial z} \right) + \dot{Q} \quad \text{Eq. (3)}$$

And the equation of heat transfer between the mould and environment is:

$$-\lambda_c \left(\frac{\partial T}{\partial n} \right) \Big|_{w1} = h_{c-m} (T_{w1} - T_{w2}) \quad \text{Eq. (4)}$$

where ρ is the density (Kg/m³) of liquid steel, C_p is latent heat (J/kg·k) of liquid steel, λ is material thermal conductivity along three main directions as x, y and z (W/(m·k)), T represents the temperature(k) of steel, t represents the time(s) and $Q=Q(x, y, z, \tau)$ represents the heat source density inside the object(W/kg), h is the heat transfer coefficient.

According to a study the relation between steel temperature and dissolved oxygen is as below ⁽⁶⁾.

$$\text{Log } [\%O] = -6320/T + 2.734 \quad \text{Eq. (5)}$$

The ladle temperature affects the oxygen level in the ladle as well. Probes that are used for the measurement of ladle temperature and the level of oxygen in ladles use two types of sensors i.e. Dissolved Oxygen measurement and Temperature of steel in ladle. Probes measure temperature and EMF followed by the measurement of oxygen using celox formula ⁽⁸⁾.

$$\text{Log } a(O) = f1 + f2 * [E + f3*T + f4*T*E]$$

Where:

E = EMF

T = temp - 1550°C (1550 °C is the temperature of the palladium bath used for calibration of the probe with +4°C deviation)

f1 = 1.3600

f2 = 0.0059

f3 = 0.5400

f4 = 0.0002

f1, f2, f3 and f4 are coefficients obtained from regression analysis by Heraeus electronite

The carbon content is calculated as follows:

$$\log \% C = f1 + f2 / T + f3 * \log a(O) \quad \text{Eq. (7)}$$

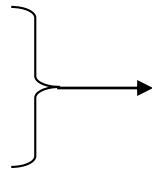
Where:

T = temp. [°C]

f1 = 2.2360

f2 = -1303

f3 = -1.0000



f1, f2 and f3 are coefficients obtained from regression analysis by Heraeus electronite.

4.1 Effect of ladle temperature (superheat) on the rate of solidification

Solidification of steel follows the square root law of solidification⁽⁹⁾, according to which the thickness of solidified steel varies linearly with the square root of time elapsed.

$$\delta = k\sqrt{\tau} \quad \text{Eq. (8)}$$

Where:

δ = the thickness of solidified steel, mm

τ = time elapsed, min

k = solidification coefficient, mm/min^{0.5}

The thickness calculated using this formula is the rim thickness if the time used in the formula is rimming duration.

The effect of superheat on the rim thickness can be explained with the help of the parameter 'k'. Solidification coefficient depends on various factors viz. the dimensions of mold, the temperature of steel superheating over the liquidus temperature, and the chemical composition of the steel cast⁽¹⁰⁾.

Variation of this parameter with superheat is shown in the following table no.1⁽¹⁰⁾

Tab.1 Established relation between Superheat of steel and solidification coefficient

Sl. No.	Superheat	Solidification coefficient
1	10	26

2	45	20
3	60	16
4	80	13
5	100	10.5

The above data is interpolated to get solidification coefficients for all the values of superheat falling between 10 to 100°C.

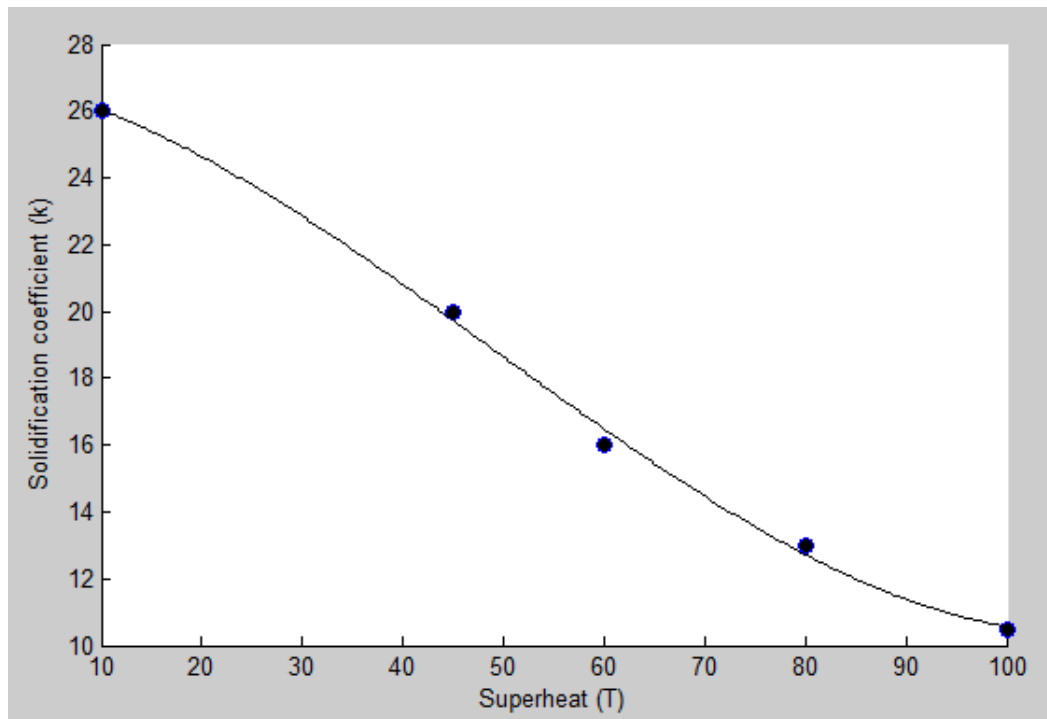


Fig.6 Variation of solidification constant (k) with superheat (T)

To visualize the variation of solidification coefficient (k) with superheat (T), the above graph has been obtained by plotting the data of table 1. The graph shows that the variation between the parameters is not strictly linear. Therefore, curve fitting has been done using MATLAB to find the relation between the two parameters. Using regression analysis, equation relating solidification coefficient and superheat has been arrived at.

The above plot shows that solidification coefficient varies with superheat according to the following equation:

$$k = 2.2e-05 * T^3 - 0.0033 * T^2 - 0.058 * T + 27$$

The following data has been obtained using the above equation.

Eq. (9)

Tab.2 Relation between Superheat of steel and solidification coefficient by Eq.9

Sl. No.	Superheat	Solidification coefficient (k)
1	10	26.000
2	20	24.690
3	30	22.880
4	40	20.800
5	50	18.600
6	60	16.390
7	70	14.310
8	80	12.500
9	90	11.088
10	100	10.200

Table 1 gives solidification coefficient for discrete values of superheat. By doing curve fitting and regression analysis, it has become possible to calculate solidification coefficient for all values of superheat. Solidification coefficient calculated, for superheats in multiples of 10 ranging from 10 - 100°C, using Eq. 9 is shown in table 2. Hence, with the help of Eq. 9, rim thickness for all values of superheat can be calculated.

EXPERIMENT CONDUCTED

The figure below (no.7) shows the design of steel ladles used to carry steel tapped from a furnace to the teeming bay⁽¹¹⁾.

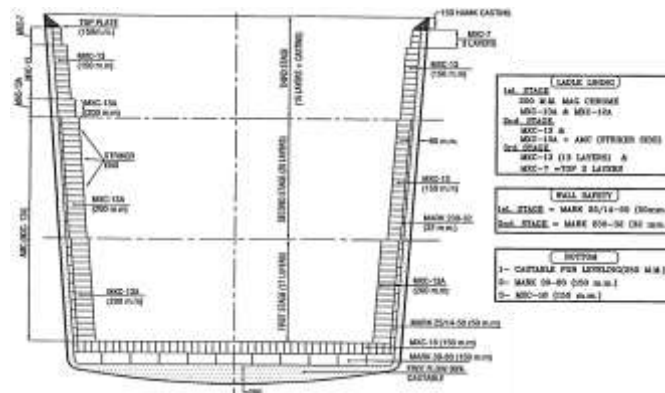


Fig.7 Steel ladle used to carry liquid steel for teeming

During the transportation of steel, heat loss takes place. Before the tapping of molten steel, ladles are preheated to prevent thermal shock on refractory bricks of the ladles. The tapping temperature is maintained around 1645°C which goes down to around 1580 - 1590°C during teeming. Various factors contribute to this loss of heat energy during the ladle cycle.

- 1) Some heat is lost to the refractory layers by conduction
- 2) Some of the heat is lost to the atmosphere by radiation. The radiated heat is reduced by the usage of slag layer and the lid.
- 3) The addition of ferroalloys also adds to the heat loss.

The thermal condition of a ladle determines the heat loss. If the heat content of the ladle is high during tapping, less heat loss from the molten steel will occur but if the heat content of the ladle is low, then heat losses from the molten steel will be higher. The construction of the ladle and its thermal properties determine the amount of heat content a ladle can carry ⁽¹²⁾.

Formulae that govern the transfer of heat through ladle wall, ladle bottom and ladle as a whole are given below ⁽¹³⁾.

Heat transfer in ladle

$$\frac{dT_m}{dt} = \frac{1}{W_m \cdot C_p(m)} [q_b(\tau) \cdot A_b + q_w(\tau) \cdot A_w + q_s(\tau) \cdot A_s] \quad \text{Eq. 10}$$

Heat transfer in refractory of ladle wall

$$\rho_{w(RH)} \cdot C_p \cdot \frac{\partial T_{w(RH)}}{\partial \tau} = \frac{1}{r} \left[\partial r \cdot \lambda_{w(RH)}(\tau) \cdot \frac{\partial T_{w(RH)}}{\partial r} \right] \quad \text{Eq. 11}$$

Heat transfer in refractory of the hearth of ladle

$$\frac{\partial T_b}{\partial \tau} = \frac{1}{\rho_b \cdot C_b(\tau)} \left[\frac{\partial}{\partial x} (\lambda_b(\tau) \frac{\partial T}{\partial x}) \right] \quad \text{Eq. 12}$$

Where:

T_m = molten steel temperature in ladle ($^{\circ}\text{C}$) ;

W_m = amount of molten steel in ladle (Kg) ;

q_b, A_b = density of heat flow into the bottom of the ladle ($\text{J}/\text{m}^2.\text{s}$), Area of the bottom (m^2) ;

q_s, A_s = density of heat flow into the slag layer ($\text{J}/\text{m}^2.\text{s}$), Area of the slag layer (m^2) ;

q_w, A_w = density of heat flow into the wall of the ladle ($\text{J}/\text{m}^2.\text{s}$), Area of the wall of the ladle (m^2) ;

$C_{p(m)}$ = Thermal capacity of molten steel ($\text{J}/\text{Kg}.\text{ }^{\circ}\text{C}$) ;

$C_{p(w)}$ = Thermal capacity of ladle wall ($\text{J}/\text{Kg}.\text{ }^{\circ}\text{C}$) ;

$C_{p(b)}$ = Thermal capacity of ladle bottom ($\text{J}/\text{Kg}.\text{ }^{\circ}\text{C}$) ;

ρ_w = Density of ladle wall (Kg/m^3) ;

ρ_b = Density of ladle bottom (Kg/m^3) ;

λ_w = Heat conduction coefficient of ladle wall ($\text{J}/\text{m.s}.\text{ }^{\circ}\text{C}$)

λ_b = Heat conduction coefficient of ladle bottom ($\text{J}/\text{m.s}.\text{ }^{\circ}\text{C}$)

τ = Time (s) ;

After the ladle reaches the teeming bay, teeming starts by opening the slide gate. The speed of teeming is altered by changing the nozzle diameter. For the sake of the experiment, the rate of filling the mould was maintained at 107.5 kg / sec.

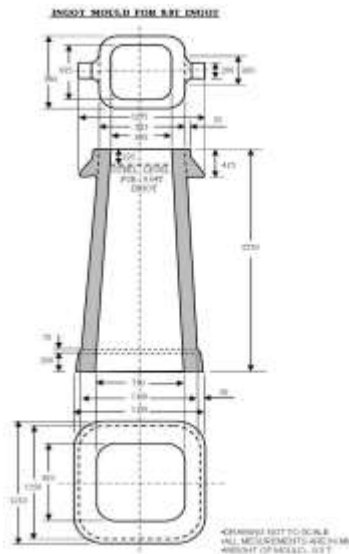


Fig.8 Size of moulds used for teeming ⁽¹¹⁾

Teeming of steel is done in moulds made of cast iron. The capacity of each individual mould is 9T with dimensions as shown in the figure above (Fig.8). Therefore, it takes around 70 – 80 seconds for each mould to get filled and the total number of moulds is 30. Chemical capping of rimming heats is done after 7 – 8 moulds get filled depending upon the scum formation over the ingot top. Hence, the rimming duration is around 11-12 mins.

OBSERVATION & RESULT

6.1 Microstructures

Microstructure of the phases over the rim propagation from mould wall towards the centre of the ingot has been studied under the optical microscope of 100X magnification with 50% HCl as etchant (fig.9). The transformation of ferrite to pearlite can be observed from this

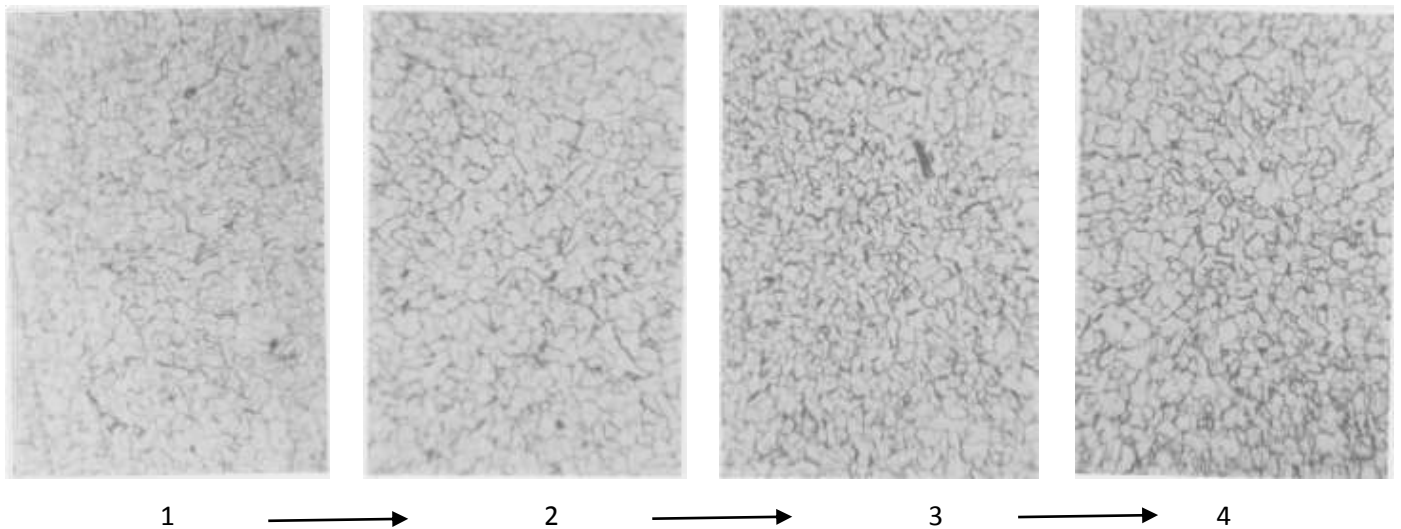


Fig. 9 Microstructure from wall towards the centre of ingot

The rim thickness of the experimental heat was found to be approximately 48 mm. The above figures show gradual transformation of the microstructure of the rim from ferrite to pearlite. Fig 9 (1) represents the microstructure of the rim near to its outer boundary, nearer to the mould wall, which is pure ferrite, whereas, fig 9 (4) represents the microstructure of the vicinity of the rim's inner boundary, towards the centre of ingot, which is a mixture of ferrite and pearlite. Transformation in microstructure of the steel at a distance of approximately 10 mm and 20 mm from position 1 towards position 4 has been shown in fig. 9(2) & 9(3).

6.2 Rim thickness obtained

Liquidus temperatures have been calculated using the following formula ⁽¹⁴⁾:

$$\text{Liquidus} = 1534 - (78 \cdot C + 7.6 \cdot \text{Si} + 4.9 \cdot \text{Mn} + 34.4 \cdot \text{P} + 38 \cdot \text{S}) \quad \text{Eq. (13)}$$

$$\text{Eq. (14)}$$

and

$$\text{Superheat} = \text{Ladle temperature} - \text{Liquidus temperature}$$

Liquidus temperature is the temperature at which an alloy starts solidifying. Ladle temperature is the temperature of molten steel just before teeming and superheat is the temperature by which the ladle temperature exceeds the liquidus temperature. From Eq. 13 it can be said that for the same grade of steel, liquidus temperature varies with chemical composition which results in varying superheat. It's imperative to take superheat into account because only proper superheat will prevent liquid steel from attaining its liquidus before the teeming process ends.

Some of the results obtained on conducting experiments is shown in Table no.3.

Tab.3 Rim thickness observed – predicted & actual

%C	%Mn	%S	%P	%Si	Ladle Temp	Superheat	Solidification coefficient (k)	Rimming duration (mins.)	Rim thickness (δ)mm	
									Predicted	Actual
0.08	0.5	0.018	0.023	0.004	1597	73.1956	13.70194262	12	47.46492	49.1439
0.09	0.47	0.015	0.023	0.005	1595	71.7222	13.98144294	12	48.43314	48.5068
0.09	0.51	0.009	0.023	0.003	1584	60.675	16.24623748	9	48.73871	46.6861
0.08	0.48	0.013	0.021	0.004	1589	64.8388	15.36282941	9	46.08849	47.6571
0.08	0.39	0.021	0.021	0.005	1589	64.7094	15.38982145	10	48.66689	51.6918
0.08	0.43	0.017	0.02	0.003	1588	63.7038	15.60066945	9	46.80201	47.9337
0.08	0.41	0.017	0.019	0.003	1585	60.5714	16.26856863	9	48.80571	49.2599

6.3 Comparison between the actual and the predicted values of rim thickness

Results of the rim thickness values obtained from prediction through equation 8&9 and actual are compared graphically (fig.10)

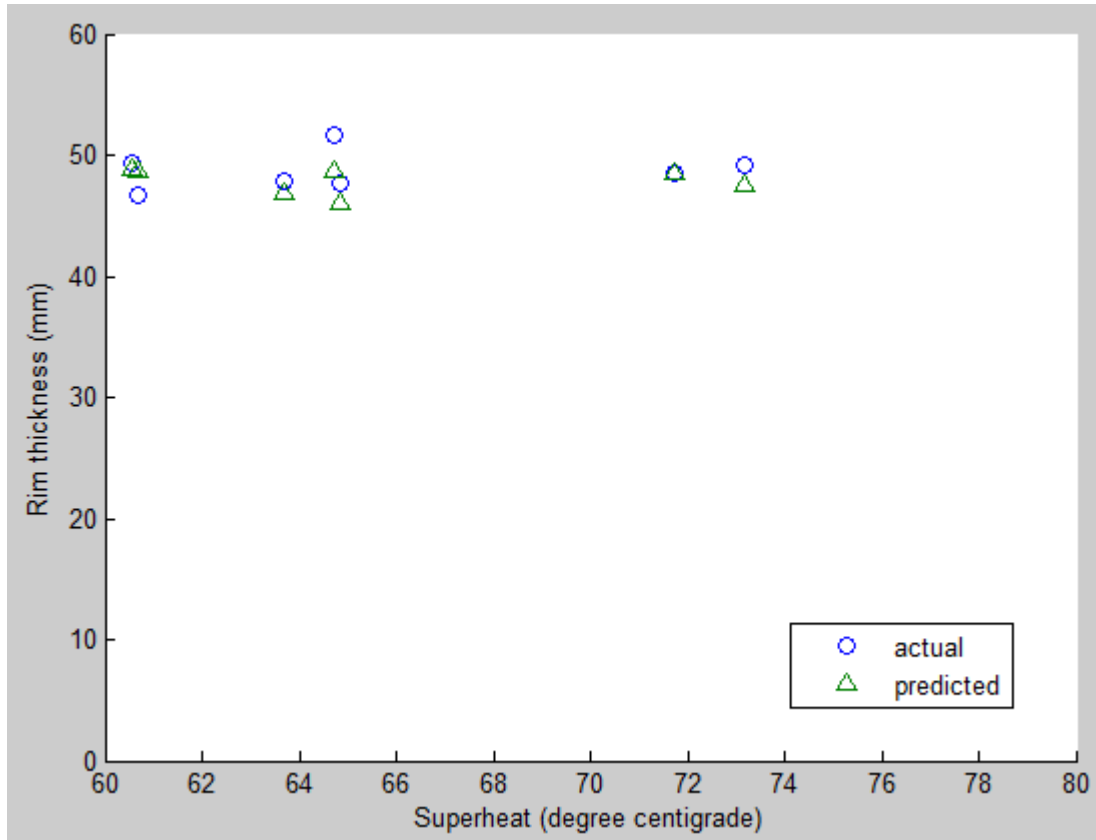


Fig.10 Comparison of predicted and actual values of rim thickness

It can be observed that predicted and theoretical values of rim thickness are very close to each other. Superheat has been taken on X – axis and Rim thickness on Y – axis. The range of deviation between the predicted and the actual values of rim thickness came to $\pm 5\%$. The deviations and the possible reasons for these have been deliberated in the discussion part.

DISCUSSION

The values observed on theoretical and actual fronts are found to be nearer to each other with a minor difference. The deviations observed are both on the positive and negative side with respect to theoretically calculated value. Equation no. 9 is pivotal in the calculation of theoretical rim thickness. It can be observed that the theoretical values of rim thickness shows increasing trend with increasing superheat which is in conformity with the theory. However, for same heat, rim thickness is not same for all the ingots, due to the loss of superheat during teeming. As the heat loss with time factor is not taken into consideration, the slight deviation from theoretical calculation from eq.9 may seep in. Therefore, maximum rim thickness for the first ingot and minimum rim thickness for the last ingot from the same heat is a common observation. Other factors which have not been taken into account in the analysis are thickness of the moulds, the temperature of moulds before teeming and the coating over mould walls. Also, the loss

of superheat is accelerated due to eroded ladle refractory lining which results into erratic results. Therefore, to some extent, the aforementioned factors contribute to the deviation between the actual and the theoretical values.

The optimum rim thickness for good results on rolling was around 45-52 mm. When the rim thickness is less than optimum then blowholes generated due to the entrapped gases in the rim become susceptible to bursting during the rolling process. If the rim thickness is more than optimum then ferrostatic pressure of entrapped gases will increase leading to chances of metal throw from the top. Moreover, due to over rim thickness oxidation of bloom surface may take place in reheating furnace leading to yield loss.

CONCLUSION

The experiments clearly showed that ladle steel temperature has a definite role in the quality of rimming steel made. Rim thickness increases with the increase in superheat. But the limitation of the ladle to handle the superheat, problem in handling the larger rims for rolling and the susceptibility of finished products to lose their shape due to over softness of the rim limits the rim thickness to an optimum level. Even-though this softness can be overcome by alloying the properties obtained may not be as comparable with pure rim. So for specific applications the pure rim formation will continue to be of importance.

ACKNOWLEDGEMENTS

We express our sincere thanks and gratitude to all the personnel who have contributed directly as well as indirectly in performing this experiment , literature survey , finding the microstructures etc..

REFERENCES

- [1] https://en.wikipedia.org/wiki/Deoxidized_steel
- [2] Dr. R.H. Tupkary, V.R. Tupkary (2011). An Introduction to Modern Steel Making.
- [3] F.R. Hutchings, G. Hanley (1974). Failures of Jib Tie-Bar Components of Tower Cranes Manufactured from Rimming Steel. British Engine Technical Report, Vol 3, as published in Source Book in Failure Analysis, American Society for Metals, 1974, p 180–208.
- [4] K N Jha, P K Sinha, S Chakraborty, Dr K P Jagannathan (1991). Commercial Production of Rimming Steels – A Suggested Approach For Tonnage Steel Plants. IE (I) Journal-MM (Sp), Vol.71, 101-114.
- [5] Standard Operating Processes guidelines of SMS-1 , Bhilai Steel Plant.
- [6] C.R.Taylor and J. Chipman (1943). TRANS .AIME, 154, 228-247
- [7] Tongjun ZHOU, Junzhan LIU, Hui LUO (Baosteel Special Steel Co, Ltd, Shanghai 200940, China) (June 2015). Process Research of Solidification in Large Ingot Casting. METEC, Düsseldorf, 15 – 19
- [8] Instruction and operating manual, Oxygen and temperature measuring unit, Multi-Lab Celox-Heraeus, Electro-Nite.
- [9] G.N. Oiks and V. Parma (JUNE 1971) .Controlling the location of primary blowholes in a rimming steel ingot...Steel in USSR , 442-447.
- [10] K. Miłkowska-Piszczek , M. Dziarmagowski , A. Buczek , J. Pióro (October 2012). The methods of calculating the solidifying strand shell thickness in a continuous casting machine. Archives of Materials Science and Engineering, Issue 2, 75-79.
- [11] Reference book of SMS-1 Bhilai Steel Plant
- [12] Muhammad Faheem (2009). A GUI for online presentation of steel and steelmaking ladle temperature data and simulation, Master's thesis E3775E.

- [13] Qing Liu, Kai Wu, Chuangji han, Kaike Cai, Heat Transfer Analysis of Molten Steel in Ladle..
<http://www.paper.edu.cn>
- [14] RDCIS, SAIL, RANCHI (2014) . Role of Ferro-alloys in Steel Making.